BULETINUL INSTITUTULUI POLITEHNIC DIN IAŞI
Publicat de
Universitatea Tehnică „Gheorghe Asachi” din Iaşi
Tomul LIX (LXIII), Fasc. 2, 2013
Secţia
ELECTROTEHNICĂ. ENERGETICĂ. ELECTRONICĂ

ON THE ROBUSTNESS OF TEXTURE CLASSIFICATION BASED ON NON-HOMOGENEOUS TWO-GRID COUPLED CELLULAR NEURAL NETWORKS

BY

PAUL UNGUREANU*

“Gheorghe Asachi” Technical University of Iaşi
Faculty of Electronics, Telecommunications and Information Technology

Received: December 17, 2012
Accepted for publication: February 18, 2013

Abstract. The two-grid coupled Cellular Neural Networks (CNN’s) have been intense studied as nonlinear and linear circuits. One of the applications that the author has already published results in conference papers is the possibility of using the double layer CNN as linear circuit and as a features extractor for textures classification application. In this paper the author, using numerical methods, has analysed the robustness of non-homogenous CNN in such application.

Key words: double layer CNN; nonlinear circuits; non-homogenous circuits; texture recognition.

1. Introduction

Cellular Neural Networks (CNN’s) are homogeneous arrays of identical and identically coupled cells (Chua & Yang, 1998). Among various types of CNN’s, one particular type is that who can produce Turing patterns (Turing, 1952). This type of CNN consists of a “sandwich” architecture: there are arrays of two-ports second order cells sandwiched between two resistive grids. Usually the CNN is a nonlinear circuit, but, also it can be used as a linear circuit (Goraş

* *e-mail*: pungureanu@etti.tuiasi.ro

& Ungureanu, 2004; Ungureanu *et al.*, 2006). In this situation, the double-layer CNN is a band-pass circular filter and has been used for images classification (Ungureanu *et al.*, 2006). In paper the robustness of filter parameters variation for textures classification has been analysed.

2 Two-Grid Coupled CNN Architecture

The double layer CNN is a non-linear circuit. The nonlinearity is represented by a nonlinear resistor which has a linear central part of characteristics. The architecture of a two-ports cell and the *i-v* characteristic of the piecewise nonlinear resistor are presented in Fig. 1 (Goraş *et al.*, 1995).

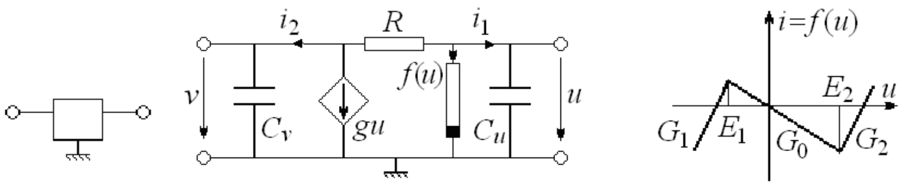

Fig. 1 – Two-ports cell and *i–u* characteristic of the piecewise nonlinear resistor.

The architectures for 1-D and 2-D CNN are presented in Fig. 2, where *u* and *v* denotes the two resistive grids.

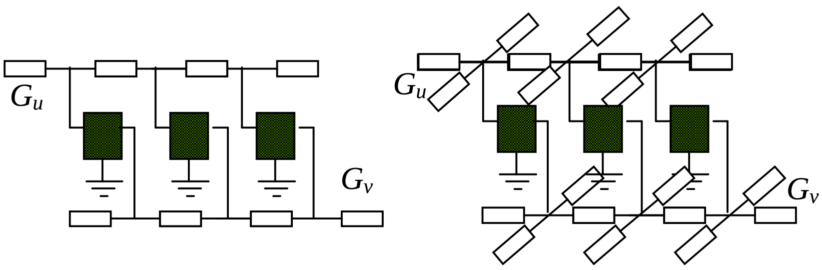

a *b*

Fig. 2 – Sketch of a 1-D two-grid coupled CNN architecture (*a*) and the way towards a 2-D array (*b*).

A cell consisting of four linear elements including a voltage controlled current source and a nonlinear resistor is described by the eqs.

$$\begin{aligned} i_1 &= f(u,v) = -G_u - f(u) + G_v, \\ i_2 &= \tilde{g}(u,v)i_1 = (G-g)u - G_v. \end{aligned} \tag{1}$$

For a circuit composed of $M \times N$ cells the eqs. that describe a 2-D CNN are (Goraş *et al.*, 1995):

$$C_u \frac{\mathrm{d}u_{ij}(t)}{\mathrm{d}t} = f(u_{ij}, v_{ij}) + G_u \nabla^2 u_{ij}, \quad (i = 0,\ldots, M-1;$$
$$C_v \frac{\mathrm{d}v_{ij}(t)}{\mathrm{d}t} = \tilde{g}(u_{ij}, v_{ij}) + G_v \nabla^2 v_{ij}, \quad j = 0,\ldots, N-1), \tag{2}$$

where $\nabla^2 x_{ij} = x_{(i+1)j} + x_{(i-1)j} + x_{i(j+1)} + x_{i(j-1)} - 4x_{ij}$ is the Laplacean.

With the notations (Goraş *et al.*, 1995):

$$\gamma = \frac{1}{C_u};\ D_u = \frac{G_u}{C_u};\ D_v = \frac{G_v}{C_v};\ g(u_{ij}, v_{ij}) = \frac{C_u}{C_v}\tilde{g}(u_{ij}, v_{ij}), \tag{3}$$

the linearization of these eqs. gives

$$\frac{\mathrm{d}u_{ij}(t)}{\mathrm{d}t} = \gamma(f_u u_{ij} + f_v v_{ij}) + D_u \nabla^2 u_{ij}, \quad (i = 0,\ldots, M-1;$$
$$\frac{\mathrm{d}v_{ij}(t)}{\mathrm{d}t} = \gamma(g_u u_{ij} + g_v v_{ij}) + D_v \nabla^2 v_{ij}, \quad j = 0,\ldots, N-1), \tag{4}$$

where f_u , f_v , g_u , g_v are the elements of the Jacobian matrix of $f(u,v)$ and $g(u,v)$, D_u and D_v are the diffusion coefficients and γ is a scaling coefficient.

Although the circuit is basically nonlinear, if no cell will reach saturation (all cell voltages are in the central linear part of the nonlinear characteristics) the circuit behaves like a linear circuit. In this situation, the analysis simplifies due to linearity and symmetry.

The system of eqs. (4) can be transformed into the following system of eqs. (Goraş *et al.*, 1995):

$$u_{ij}(t) = \sum_{m=0}^{M-1}\sum_{n=0}^{N-1} \Phi_{MN}(i,j,m,n)\hat{u}_{mn}(t),$$
$$v_{ij}(t) = \sum_{m=0}^{M-1}\sum_{n=0}^{N-1} \Phi_{MN}(i,j,m,n)\hat{v}_{mn}(t), \tag{5}$$
$$(i = 0,\ldots,M-1;\ j = 0,\ldots,N-1),$$

where $\Phi_{MN}(i, j, m, n)$ are eigenfunctions (which depend on the boundary conditions) of the 2-D Laplacean *i.e.*, $\nabla^2\Phi_{MN}(i,j,m,n) = -k_{mn}^2\Phi_{MN}(i,j,m,n)$ and $-k_{mn}^2$ are the eigenvalues, proportional to the square (or sum of squares) of sine functions (Goraş *et al.*, 1995).

The solution of the 2-D CNN equations is (Goraş *et al.*, 1995):

$$
\begin{aligned}
&u_{ij}(t)=\sum_{m=0}^{M-1}\sum_{n=0}^{N-1}(a_{mn}\mathrm{e}^{\lambda_{mn1}t}+b_{mn}\mathrm{e}^{\lambda_{mn2}t})\Phi_{MN}(i,j,m,n),\\
&v_{ij}(t)=\sum_{m=0}^{M-1}\sum_{n=0}^{N-1}(c_{mn}\mathrm{e}^{\lambda_{mn1}t}+d_{mn}\mathrm{e}^{\lambda_{mn2}t})\Phi_{MN}(i,j,m,n),\\
&\qquad (i=0,\dots,M-1;\;\; j=0,\dots,n-1).
\end{aligned}
\tag{6}
$$

For ring conditions

$$
\begin{cases} u_{i,M}=u_{i,0} \\ u_{i,-1}=u_{i,M-1} \end{cases} \text{and} \begin{cases} u_{M,j}=u_{0,j} \\ u_{-1,j}=u_{M-1,j} \end{cases}, \text{ for } u_{i,j} \text{ layer}
$$

and

$$
\begin{cases} v_{i,M}=v_{i,0} \\ v_{i,-1}=v_{i,M-1} \end{cases} \text{and} \begin{cases} v_{M,j}=v_{0,j} \\ v_{-1,j}=v_{M-1,j} \end{cases}, \text{ for } v_{i,j} \text{ layer,}
$$

the eigenvectors are the complex exponentials of Discreet Fourier Transform (Goraş *et al.*, 1995)

$$
\Phi_{MN}(i,j,m,n)=\mathrm{e}^{\mathrm{j}\frac{2\pi}{M}mi}\,\mathrm{e}^{\mathrm{j}\frac{2\pi}{N}nj}.
$$

The values λ_{mn1} and λ_{mn2} represent the roots of the characteristic polynomial obtained from differential eqs. (4). Making the change of variable and taking the scalar product of both sides of the eqs. (4) the dynamics of the 2-D CNN is described by the following set of pairs of decoupled linear eqs. (Goraş *et al.*, 1995):

$$
\begin{bmatrix} \dot{\hat{u}}_{mn} \\ \dot{\hat{v}}_{mn} \end{bmatrix} = \left(\gamma \begin{bmatrix} f_u & f_v \\ g_u & g_v \end{bmatrix} - k_{mn}^2 \begin{bmatrix} D_u & 0 \\ 0 & D_v \end{bmatrix} \right) \begin{bmatrix} \hat{u}_{mn} \\ \hat{v}_{mn} \end{bmatrix},\ (m=0,\dots,M-1;\ n=0,\dots,N-1). \tag{7}
$$

Thus, the set of $2 \times M \times N$ coupled differential eqs. in the u and v variables transforms into M sets of pairs of second order differential eqs. in the new variables: the amplitudes of the spatial components of the voltages (Goraş *et al.*, 1995)

$$
\begin{aligned}
&\lambda_{mn}^2+\lambda_{mn}[k_{mn}^2(D_u+D_v)-\gamma(f_u+g_v)]+D_uD_vk_{mn}^4-\\
&-\gamma(D_vf_u+D_ug_v)k_{mn}^2+(f_ug_v-f_vg_u)=0,\\
&(n=0,\dots,N-1;\; m=0,\dots,M-1).
\end{aligned}
\tag{8}
$$

As for every linear circuit, in order to have an unstable CNN, some eigenvalues λ_{mn} with positive real part, must exist (Goraş *et al.*, 1995)

$$\Re e\left\{\lambda_{1,2}(k_{mn}^2)\right\} = \Re e\left\{\begin{array}{l}\gamma\dfrac{f_u+g_v}{2} - k_{mn}^2\dfrac{D_u+D_v}{2} + \\ \hline + \sqrt{\left[\gamma\dfrac{(g_v-f_u)}{2} + k_{mn}^2\dfrac{D_u-D_v}{2}\right]^2 + \gamma^2 f_v g_u}\end{array}\right\}. \tag{9}$$

Thus a band of unstable modes will result. The values of *m* and *n* for which the real part of λ_{mn} is positive, will correspond to the band of stable modes. So, the conditions that must be fulfilled, in order to have a band of unstable modes, will result (Goraş *et al.*, 1995)

$$\begin{aligned} & f_u + g_v < 0, \\ & f_u g_v - f_v g_u > 0, \\ & D_v f_u + D_u g_v > 0, \\ & (D_v f_u - D_u g_v)^2 + 4 D_u D_v f_v g_u > 0 \, . \end{aligned} \tag{10}$$

For specified values of CNN parameters, the variation of the real part of the roots can be represented. Two dispersion curves as those presented in Fig. 3 for $f_u = 0.1$, $f_v = -1$, $g_u = 0.1$, $g_v = -0.2$, $D_u = 1$, will result.

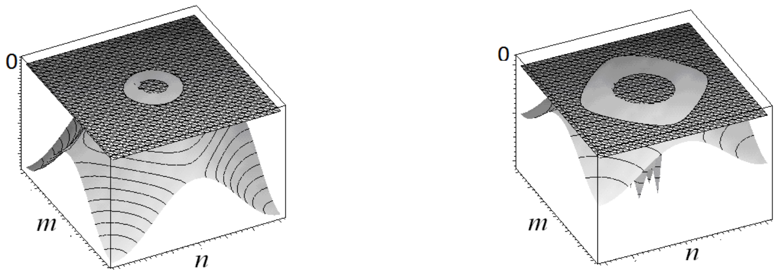

$D_v = 65, \gamma = 12$ $D_v = 50, \gamma = 45$

Fig. 3 – Typical dispersion curve.

3. Linear Filtering

It has been shown that Turing patterns appear if there is a band of unstable modes having positive eigenvalues, which will grow in time until some nonlinearity limits their growth (Goraş & Ungureanu, 2004).

As already mentioned, in order to have a linear two-grid CNN, no cell should reach saturation (all cell voltages are in the central linear part of the nonlinear characteristics) (Goraş *et al.*, 1995; Goraş & Ungureanu, 2004). This happens if the transient toward a pattern is frozen at a given time, t_0, before any cell nonlinearity has been reached. In such a case, the CNN behaves as a linear spatial filter having a spatial frequency characteristic dependent on t_0.

Considering $v_{mn} = 0$, the behavior of the network can be described by associating a time varying spatial transfer function, as a ratio between the amplitudes of the modes at a given moment, t_0, and their initial amplitudes (Ungureanu *et al.*, 2006)

$$H_{mn}(t_0) = \frac{\hat{u}_{mn}(t_0)}{\hat{u}_{mn}(0)} = \frac{(\lambda_{mn1} - \gamma f_u + D_u k_{mn}^2)\mathrm{e}^{\lambda_{mn2} t_0} - (\lambda_{mn2} - \gamma f_u + D_u k_{mn}^2)\mathrm{e}^{\lambda_{mn1} t_0}}{\lambda_{mn1} - \lambda_{mn2}}.$$

The frequency characteristic of the two-grid CNN's described by the following parameters: $f_u = 0.1$, $f_v = -1$, $g_u = 0.1$, $g_v = -0.2$, $D_u = 1$, $D_v = 50$, $\gamma = 38$ and calculated for the moment, $t_0 = 1$ is presented in Fig. 4.

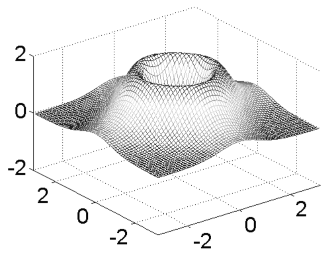

Fig. 4 – Frequency characteristic of a two-grid CNN's at the moment 1.

Using this result, a band of band-pass filters can be designed, which have been already used as features extractors for textures classification purposes. The classification method is a classical one and has been presented by Ungureanu *et al.*, 2006 and Alecsandrescu *et al.*, 2008. It consists of five band-pass filters used for feature extraction (for every filtered image, the L2 norm has been calculated). It will result a five elements feature vector, which represents that type of texture. For classification, the distance between features vectors has been calculated and the nearest neighbor algorithm has been used. In Fig. 5, the amplitude characteristics of the five filters are presented. For comparison the corresponding ideal circular also, is presented.

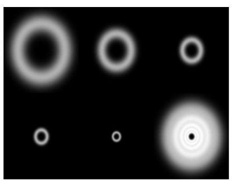

a

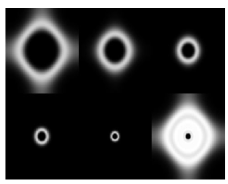

b

Fig. 5 – *a* – Circular ideal filter characteristics and their superposition; *b* – corresponding filter characteristics implemented with homogeneous CNN's.

For the five two-grid CNN's the following parameters have been used:

Filter 1	$f_u = 0.1, f_v = -1, g_u = 0.1, g_v = -0.2, D_u = 1, D_v = 50, \gamma = 69, t_0 = 2.3$
Filter 2	$f_u = 0.1, f_v = -1, g_u = 0.1, g_v = -0.2, D_u = 1, D_v = 50, \gamma = 33, t_0 = 2.5$
Filter 3	$f_u = 0.1, f_v = -1, g_u = 0.1, g_v = -0.2, D_u = 1, D_v = 50, \gamma = 14, t_0 = 4.5$
Filter 4	$f_u = 0.1, f_v = -1, g_u = 0.1, g_v = -0.2, D_u = 1, D_v = 50, \gamma = 5.5, t_0 = 11$
Filter 5	$f_u = 0.1, f_v = -1, g_u = 0.1, g_v = -0.2, D_u = 1, D_v = 50, \gamma = 2, t_0 = 30$

For analysis, the Brodatz database (Brodatz, 1966) has been used. The data base consists of 16 texture types having the resolution 128 × 128. Each texture type will be represented by 28 different images, each image being rotated with 10 angles (0º, 20º, 30º, 45º, 60º, 70º, 90º, 120º, 135º, 150º). The 16 textures and the 10th texture rotated with 10 angles are presented in Fig. 6.

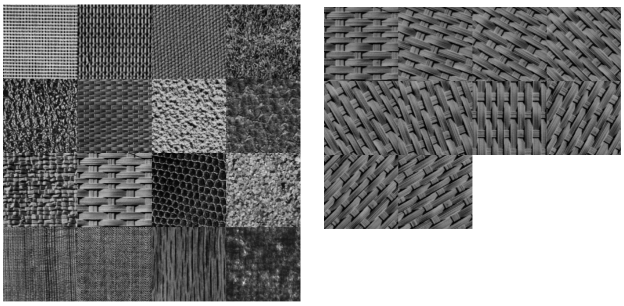

Fig. 6 – Textures from Brodatz database.

The results have been reported by Ungureanu *et al.*, 2006. For homogeneous CNN the classification performance was 97.37%.

4. Nonhomogenous Linear Two-Grid CNN's

The effect on classification performances of CNN parameters variations has been studied. In such a case, the system of eqs. (4), becomes

$$\begin{aligned} &\frac{\mathrm{d}u_{ij}(t)}{\mathrm{d}t} = \gamma(f_{u_{ij}} u_{ij} + f_{v_{ij}} v_{ij}) + D_u \nabla^2 u_{ij}, \\ &\frac{\mathrm{d}v_{ij}(t)}{\mathrm{d}t} = \gamma(g_{u_{ij}} u_{ij} + g_{v_{ij}} v_{ij}) + D_v \nabla^2 v_{ij}, \\ &\quad (i = 0, \ldots, M-1; j = 0, \ldots, N-1).. \end{aligned} \tag{11}$$

The frequency responses for a realization of the nonhomogeneous filter for 10% variation are presented in Fig. 7. The responses have been obtained using 2-D signal with zeros and just one nonzero element (*e.g.* discrete Dirac). The CNN has been simulated using Euler method to solve differential eqs.

From the Fig. 7 it can be observed that the parameters variance affects especially the filters with high frequency bands.

In order to analyse the performances of the circuit a Gaussian distribution of CNN parameters with variance 5%, 10%, 20% of the parameters nominal value has been used.

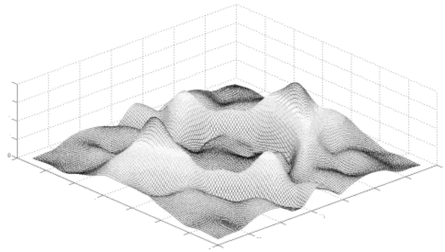

Filter 1

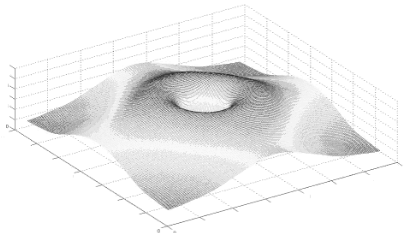

Filter 2

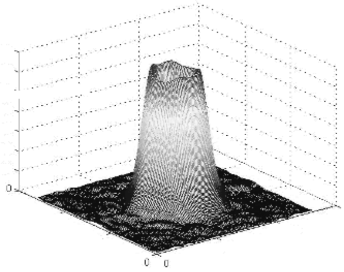

Filter 3

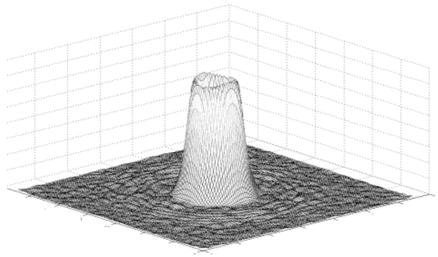

Filter 4

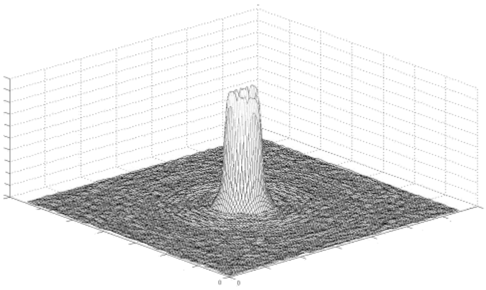

Filter 5

Fig. 7 – Frequency characteristics for a nonhomogenous 10% variation of CNN parameters.

Texture classification system performances are presented in Fig. 8. For 5% and 10% the results are approximately the same as those for homogenous CNN. For 20% parameters variation, the performances have decreased with 3%. In order to use two-grid CNN's for textures classification, the circuit must have a band of unstable modes. Otherwise, after loading the initial conditions, the evolution of the capacitors voltage will evolve towards zero. So, it is important to make sure that if the homogenous CNN is unstable, the non-homogenous one it is also unstable. Unfortunately where there are not conditions for unstable two-grid CNN's like whose from eqs. (10).

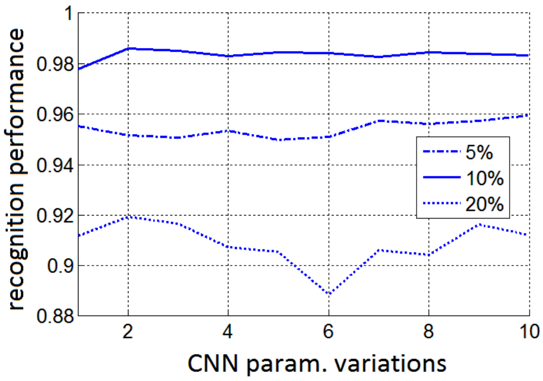

Fig. 8 – Recognition performance for ten CNN's realizations.

One solution is the statistical analysis: for a large number of CNN's parameters variations the circuit must remain unstable (*e.g.* the largest real part of the eigenvectors must be positive).

Fig. 9 presents the maxima eigenvalues real part; obtained through simulations, for 1,000 CNN's parameters variations. For each filter, the matrix eigenvalues correspond to the system of differential eqs.

$$\begin{bmatrix} \frac{\mathrm{d}u_{00}(t)}{\mathrm{d}t} \\ \vdots \\ \frac{\mathrm{d}u_{ij}(t)}{\mathrm{d}t} \\ \vdots \\ \frac{\mathrm{d}u_{MN}(t)}{\mathrm{d}t} \\ \frac{\mathrm{d}v_{00}(t)}{\mathrm{d}t} \\ \vdots \\ \frac{\mathrm{d}v_{ij}(t)}{\mathrm{d}t} \\ \vdots \\ \frac{\mathrm{d}v_{MN}(t)}{\mathrm{d}t} \end{bmatrix} = U_{2\text{-D CNN}} \begin{bmatrix} u_{00}(t) \\ \vdots \\ u_{ij}(t) \\ \vdots \\ u_{MN}(t) \\ v_{00}(t) \\ \vdots \\ v_{ij}(t) \\ \vdots \\ v_{MN}(t) \end{bmatrix}, \text{ where } \begin{cases} i = 0,\ldots, M-1; \\ j = 0,\ldots, N-1. \end{cases} \tag{12}$$

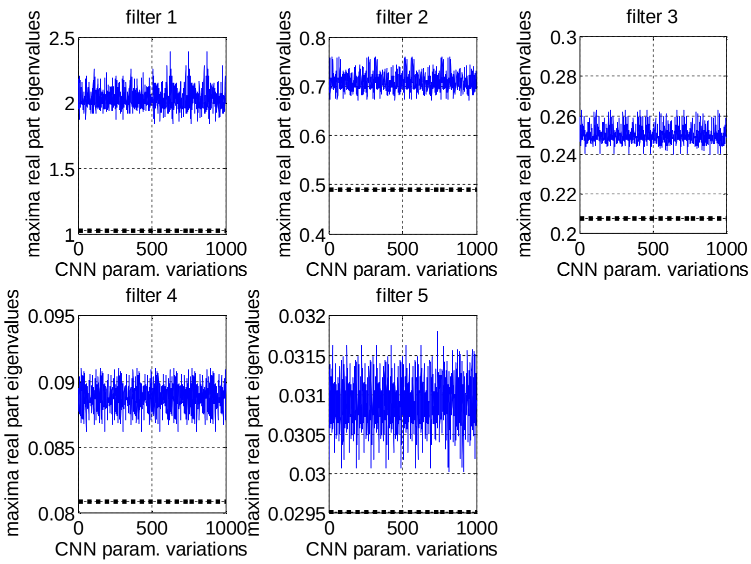

Fig. 9 – The real part eigenvalues maxima for each of five filters.

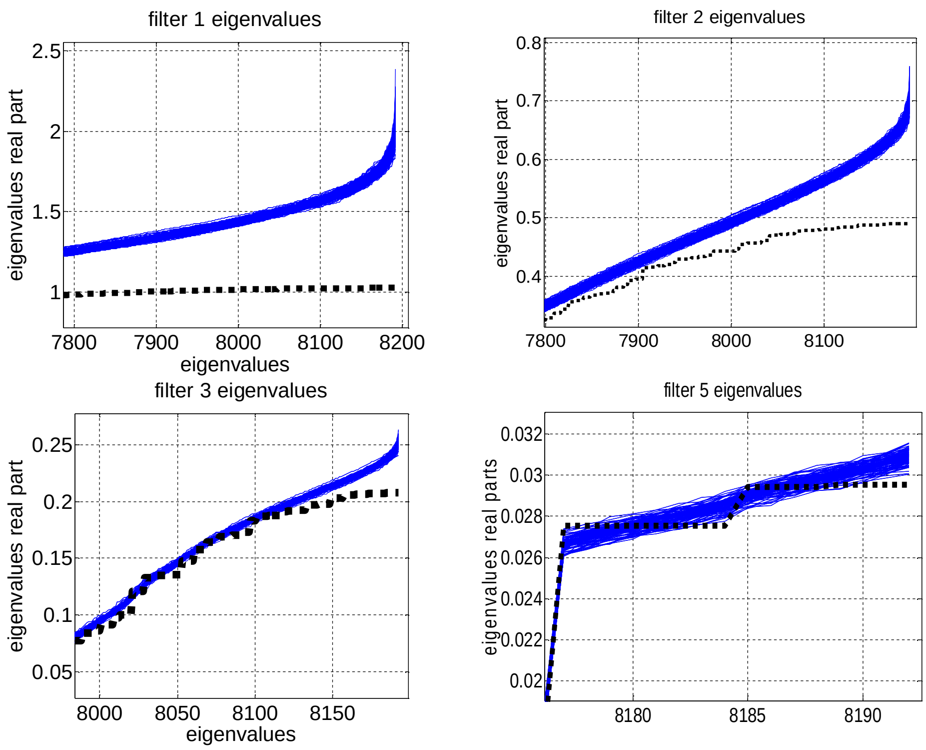

Fig. 10 – Eigenvalues real part for homogeneous and non-homogeneous 2-D CNN.

The matrix $U_{2-\mathrm{D\,CNN}}$ has been obtained from the system of differential eqs. (11). Has been also plotted, using dotted line the maxima eigenvalues real part for the homogenous CNN. From these figures can be observed that, for 10% variations of 2-D CNN parameters, the CNN is unstable (the maxima of eigenvalues real parts are all positive).

In Fig. 10, the largest values of eigenvalues real parts for homogenous (dotted line) and non-homogenous CNN (solid line) are presented. From the simulations it can be observed that the biggest non-homogenous CNN eigenvalues real parts are larger than homogenous CNN eigenvalues real parts. This observation can ensure that an implementation of a designed unstable double layer CNN will, also, be unstable.

5. Conclusions

In paper the robustness of double-layer CNN parameters variation for textures classification has been presented. Although there isn't an analytical method for specify the stable or unstable character of non-homogenous double-layer CNN, through simulations has been observed that for 10% parameter variations, the circuit is unstable and can be used for textures classification applications.

REFERENCES

Alecsandrescu I., Ungureanu P., Goraş L., *Nonhomogeneous CNN's and their Use for Texture Classification*. 9th Symp. on Neural Network Appl. in Electr. Engng., NEUREL 2008, September 25–27, 2008, Belgrade, Serbia, 153-156.

Brodatz P., *Textures: A Photographic Album for Artists and Designers*. Dover, New York, 1966.

Chua L.O., Yang L., *Cellular Neural Networks: Applications*. IEEE Trans. Circ. Syst., **35**, *10*, 1273-1290 (1988).

Chua L.O., Yang L., *Cellular Neural Networks: Theory*. IEEE Trans. Circ. Syst., **35**, *10*, 1257-1272 (1988).

Goraş L., Chua L. O., *Turing Patterns in CNN's* – Part II: *Equations and Behaviors*. IEEE Trans. Circ. Syst., **42**, 612-626 (1995).

Goraş L., Chua L.O., Leenaerts D.M.W., *Turing Patterns in CNN's* – Part I: *Once Over Lightly*. IEEE Trans. Circ. Syst., **42**, 602-611 (1995).

Goras L., Ungureanu P., *On the Possibilities of Using Two-Grid Coupled CNN's for Face Feature Extraction*. IEEE Symp.on Cellular Neural Networks a. Appl., CNNA 2004, Budapest, Hungary, July 22-24, 2004, 381-386.

Goraş L., Vornicu I., Ungureanu P., *Topics on Cellular Neural Networks*, chapter in *Handbook on Neural Information Processing*, M. Bianchini, M. Maggini, L. Jain (Eds.), Elsevier, Springer Verlag, 2013.

Murray J.D., *Mathematical Biology*. Springer-Verlag, Berlin-Heidelberg, 1993

Turing A.M., *The Chemical Basis of Morphogenesis*. Phil. Trans. Roy. Soc. London, **B 237**, 37-72 (1952).

Ungureanu P., David E., Goraş L., *On Rotation Invariant Texture Classification Using Two-Grid Coupled CNNs.* 8th Seminar on Neural Network Appl. in Electr. Engng., NEUREL-2006, Belgrade, September 25-27, 2006, 33-36.

ANALIZA ROBUSTEȚII CLASIFICĂRII TEXTURILOR FOLOSIND REȚELE NEURONALE CELULARE DE TIP DUBLU STRAT NEOMOGENE

(Rezumat)

Se prezintă rezultatele obținute de autor în ceea ce priveşte stabilitatea circuitelor neurale celulare (RNC) de tip dublu strat neomogene. Autorul a publicat deja în alte articole rezultatele obținute în ceea ce priveşte posibilitatea utilizării RNC de tip dublu strat liniare ca extractori de trăsături în aplicații de clasificare a texturilor. Pentru ca o RNC de tip dublu strat să poată fi folosită în astfel de aplicații trebuie să-şi păstreze caracterul instabil chiar dacă circuitul este neomogen (parametrii celulei variază de la o celulă la alta). În literatura de specialitate nu există deocamdata publicată o metodă analitică de a stabili caracterul stabil sau instabil al unei RNC de tip dublu strat neomogen. În acest articol, pentru analiza stabilitații s-au utilizat metode numerice.